

Effective flexural rigidities for RC beams and columns with steel fiber

Habib Akbarzadeh Bengar^{*1}, Mohammad Asadi Kiadehi^{1a},
Javad Shayanfar^{2b} and Maryam Nazari^{3c}

¹Department of Civil Engineering, University of Mazandaran, Babolsar, Iran

²Department of Civil Engineering, University of Minho, guimaraes, Portugal

³Department of Civil Engineering, California State University, Fresno, CA, USA

(Received March 9, 2019, Revised December 15, 2019, Accepted December 27, 2019)

Abstract. Influences of different variables that affect the effective flexural rigidity of reinforced concrete (RC) members are not considered in the most seismic codes. Furthermore, in the last decades, the application of steel fibers in concrete matrix designs has been increased, requiring development of an accurate analytical procedure to calculate the effective flexural rigidity of steel fiber reinforced concrete (SFRC) members. In this paper, first, a nonlinear analytical procedure is proposed to calculate the SFRC members' effective flexural rigidity. The proposed model's accuracy is confirmed by comparing the results obtained from nonlinear analysis with those recorded from the experimental testing. Then a parametric study is conducted to investigate the effects of different parameters such as varying axial load and steel fiber are then investigated through moment-curvature analysis of various SFRC (normal-strength concrete) sections. The obtained results show that increasing the steel fiber volume percentage increases the effective flexural rigidity. Also it's been indicated that the varying axial load affects the effective flexural rigidity. Lastly, proper equations are developed to estimate the effective flexural rigidity of SFRC members.

Keywords: effective flexural rigidity; SFRC members; varying axial load; fiber method analysis

1. Introduction

Reinforced concrete (RC) structures respond nonlinearly during extreme loads such as earthquakes. Nonlinear behavior of the structures should be evaluated through nonlinear analysis, which is often time-consuming. Many codes suggest the designers to perform an equivalent elastic analysis to calculate displacements and forces of the elements by using their alternative linear characteristics.

One of the most important parameters that is used in the elastic analysis is the effective flexural rigidity of the members, which ultimately affects the load-displacement curve's initial slope. Various parameters such as cracking and nonlinearity of the materials may result in a change in the RC members' effective flexural rigidity (Mirza and Tikka 1999). Several research studies were performed to investigate the RC members' effective flexural rigidity. Kumar and Singh (2010) investigated the effect of concrete compressive strength on the RC members' effective flexural rigidity. The results indicated that the RC members' effective flexural rigidity depended on the concrete compressive stress. Pauley and priestly (1992) evaluated various parameters which influenced on the RC members' effective flexural rigidity and recommended the average

value for any level of axial load. Many codes such as ACI and CSA outlined different approaches to consider the RC members' effective flexural rigidity. In ACI-318 (2014), the effective flexural rigidity of the members relate to the type of the element; for RC columns, in the braced frames and the free sway frames, these values are $E_c I_g$ and $0.7 E_c I_g$, respectively, where the effective flexural rigidity of RC beams are smaller and equal to $0.5 E_c I_g$ and $0.35 E_c I_g$. CSA A23.3 (2014) proposed $0.35 E_c I_g$ for RC beams and $0.7 E_c I_g$ for RC columns.

One of the most significant issues with the application of plain concrete is its brittle failure due to compression loads and cracking due to the tension loads. In order to address these concerns, researchers proposed to use steel fibers (SF) into the concrete matrix design. They indicated that this approach may enhance the mechanical features of plain concrete such as compression strength and the corresponding strain (Abbass *et al.* 2018; Campione and Mangiavillano 2008, Zarrin and Khoshnoud 2016, Jang and Yun 2018). Also it was reported that application of SF increased the ductility and tensile strength of plain concrete (Moradi *et al.* 2016, Chalioris and Panagiotopoulos 2018, Gribniak *et al.* 2012; Zarrin and Khoshnoud 2016, Xu *et al.* 2017, Bae *et al.* 2017, Lee *et al.* 2017). Some researchers investigated the behavior of RC beams, columns and shear wall with SF (Campion and Mangivillano 2008, Ashour *et al.* 2000, Germano *et al.* 2013 and Gao *et al.* 2018, Qissab and Salman 2018). Campione and Mangivillano (2008), investigated the effects of SF on nonlinear behavior of RC beams and indicated a higher effective flexural rigidity of RC beams with SF compared to RC beams. Ashour *et al.*

*Corresponding author, Ph.D.

E-mail: h.akbarzadeh@umz.ac.ir

^aM.Sc Student

^bPh.D. Student

^cPh.D.

(2000) performed experimental tests on the beams to investigate the effect of SF, longitudinal bars percentage, and concrete compressive strength on the flexural performance of RC beams with SF. The results indicated that by increasing in SF volume percentage and longitudinal bar, the effective flexural rigidity increased. To predict the behavior of RC elements with SF, an accurate analytical procedure is needed with the consideration of all of the parameters that significantly affect their nonlinear behavior, such as the axial load. High axial load result in more stiffness. In structural frames, especially in exterior columns, the variation of the axial load due to the lateral force should be considered. This will result in an additional compression axial load in one side of the frame and tensional axial load in the other side of the frame. Experimental tests indicated that the columns under varying axial load showed totally different values for strength, ductility and stiffness in comparison to those under constant axial load (Abrams 1987, Ousalem *et al.* 2002, Sezen 2002).

In this paper, SF effects on the RC beams and columns' effective flexural rigidity is investigated through moment-curvature analysis considering the varying axial load. Also, to compute the RC (normal-strength concrete) beams and columns' effective flexural rigidity with SF, proper equations are then proposed.

2. Proposed models for effective flexural rigidity

ACI-318 (2014) and CSA A23.3 (2014) recommended different α_{eff} (the reduction factor which is the ratio of effective rigidity to the rigidity based on the gross concrete features (I_e/I_g)) for RC members, as summarized in Table 1. Paulay and Priestly (1992) proposed α_{eff} for both columns and beams. They also suggested an average values, as presented in Table 1. According to this table, the effective flexural rigidity depends on the axial load value. It also shows that by increasing the axial load value the effective flexural rigidity is increased.

The results of a research study conducted by Avşar *et al.* (2014) indicated that the concrete compression strength as well as the longitudinal bars percentage may vary the effective flexural rigidity of RC elements in addition to the axial load value. Accordingly, Eqs. (1) and (2) were proposed to calculate α_{eff} of RC columns and beams.

For RC columns

$$\alpha_{eff} = 0.062 + 0.0022 \times f_c + 0.854 \times \frac{N}{A_g f_c} + 10.802 \times \rho_s \quad \text{for } \frac{N}{A_g f_c} > 0.3 - 1.91 \rho_s$$

$$\alpha_{eff} = 0.257 - 0.0033 \times f_c + 0.602 \times \frac{N}{A_g f_c} + 13.874 \times \rho_s \quad \text{for } \frac{N}{A_g f_c} \leq 0.3 - 1.91 \rho_s \quad (1)$$

For RC beams

$$\alpha_{eff} = 0.271 - 0.0064 \times f_c + 0.12 \times \frac{\rho'}{\rho_{st}} + 37.895 \times \rho_{st} \quad (2)$$

Table 1 α_{eff} values recommended by Paulay and Priestly, ACI-318 and CSA A23.3

	Paulay and Priestly	Paulay and Priestly (average)	ACI-318 (2014)	CSA A23.3 (2014)
Rectangular beams	0.3-0.5	0.4	0.35 (FSF)* 0.5 (BF)*	0.35
Columns, $P > 0.5 f_c A_g$	0.7-0.9	0.8	0.7 (FSF) 1 (BF)	0.7
Columns, $P = 0.2 f_c A_g$	0.5-0.7	0.6	0.7 (FSF) 1 (BF)	0.7
Columns, $P = -0.05 f_c A_g$	0.3-0.5	0.4	0.7 (FSF) 1 (BF)	0.7

*FSF and BF stand for free sway frames and braced frames; P is axial load; f_c is concrete compressive strength; A_g is gross area of cross-section

where f'_c is concrete peak stress in compression, N is axial load value, ρ_s is longitudinal bars percentage, ρ_{st} and ρ' are tension and compression bar percentage and A_g is the cross-section gross area.

Effective flexural rigidity for RC beams and columns can be determined from moment-curvature analysis using Eq. (3) (Avşar *et al.* 2014, Chen *et al.* 2017).

$$E_c I_e = \frac{M_y}{\phi_y} \quad (3)$$

where M_y is yield moment and ϕ_y is yield curvature which obtained from moment-curvature curve at which tensile reinforcement attains the yield strain or the concrete extreme compression fiber attains a strain of 0.002, whichever occurs first (Avşar *et al.* 2014).

Aforementioned, the axial load especially in exterior columns is not constant during seismic load, which should be taken into account while estimating the flexural rigidities of these elements. Also the impacts of using SF in RC beams and columns is not considered in the above-mentioned equations. Therefore, to modify the relations for the estimation of the effective flexural rigidity, the influences of SF and varying axial load should be considered.

3. Compression and tension stress-strain model for SFRC

3.1 Behavior of SFRC in compression

Campione and Mangiavillano (2008) proposed a model for stress-strain relationship of unconfined SFRC in compression, as presented in Eqs. (4)-(6)

$$f_{cf} = f'_c + 6.913F \quad (4)$$

$$\varepsilon_{of} = \varepsilon_0 + 0.00192.F \quad (5)$$

$$F = \beta v_f \frac{L_f}{D_f} \quad (6)$$

where f'_c and ϵ_0 are, respectively, concrete compressive stress and the corresponding strain, f_{cf} and ϵ_{of} are, respectively, steel fiber concrete compressive stress and the corresponding strain. According to these equations, the characteristics of SFRC mostly depends on the fiber factor, F . As it can be seen in Eq. (6), the SF aspect ratio affects the fiber factor where D_f and L_f are the diameter and length of SF, v_f is SF volume percentage, and β is the factor relates to SF shape assumed as 1 for deformed and 0.5 for straight fibers. According to Campione and Mangiavillano (2008), a model was proposed to calculate SFRC stress-strain curve, as presented below

$$\sigma = f_{cf} \frac{A \frac{\epsilon}{\epsilon_{0f}} + (D-1) \left(\frac{\epsilon}{\epsilon_{0f}} \right)^2}{1 + (A-2) \frac{\epsilon}{\epsilon_{0f}} + D \left(\frac{\epsilon}{\epsilon_{0f}} \right)^2} \quad (7)$$

in which $A = E_c / E_0$, E_0 is the compressive stress secant modulus described as $E_0 = f_{cf} / \epsilon_{of}$ and E_c is the modulus of elasticity of concrete. Moreover, parameter D was defined as follows

$$D = 0.3136 + 0.175F \quad (8)$$

3.2 Confinement effect in SFRC

In this paper, for the confined region of RC and SFRC section, proposed relations by Mander *et al.* (1998) and Wang and Restrepo (2001) were followed with some modifications. The confined concrete stress-strain relationship can be defined as below

$$f_c = \frac{f_{cc} x^r}{r - 1 + x^r} \quad (9)$$

$$f_{cc} = \alpha_1 \alpha_2 f'_c \quad (10)$$

$$\alpha_1 = \left(2.254 \sqrt{1 + \frac{7.94 F_l}{f'_c}} - 2 \frac{F_l}{f'_c} - 1.254 \right) \quad (11)$$

$$\alpha_2 = \left(1.4 \frac{f_l}{F_l} - 0.6 \left(\frac{f_l}{F_l} \right)^2 - 0.8 \right) \sqrt{\frac{F_l}{f_l}} + 1 \quad (12)$$

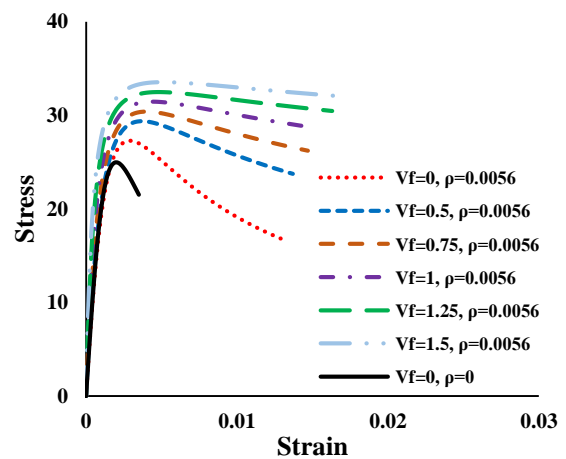
$$\epsilon_{cc} = \epsilon_0 \left[1 + 5 \left(\frac{f_{cc}}{f_{c0}} - 1 \right) \right] \quad (13)$$

where α_1 is the compressive stress incensement factor when the concrete subjected to a tri-axial stress with equal confining stresses in two perpendicular side; α_2 is the concrete compressive stress reduction factor confined with unequal lateral confining pressures, in two perpendicular

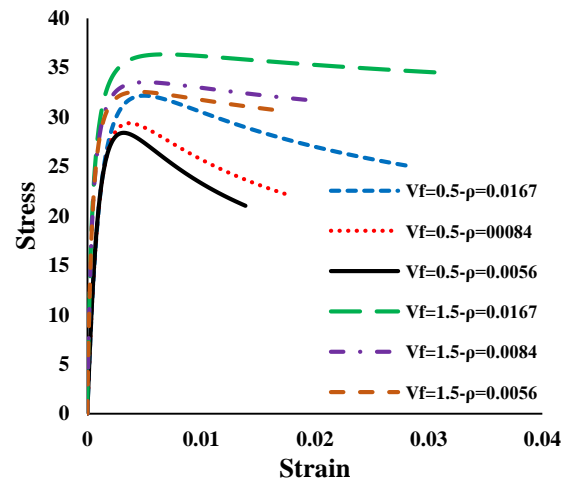
side. f_{cc} and ϵ_{cc} are, respectively, peak compressive stress of confined concrete and the corresponding strain, E_{sec} is secant modulus of confined concrete, F_l and f_l are maximum and minimum lateral confinement pressure. The confined concrete ultimate strain was considered according to Eq. (14) which was developed by priestly *et al.* (1996).

$$\epsilon_{cu} = 2\epsilon_0 + \frac{1.4 f_{yh} \rho \epsilon_{sm}}{f_{cc}} \quad (14)$$

where ρ is the volume ratio of stirrups and ϵ_{sm} is steel material ultimate strain of stirrup. Putting the SFRC peak stress f_{cf} and the corresponding strain ϵ_{of} into Eqs. (10), (13) and (14), stress-strain relationship for confined SFRC can be calculated. Fig. 1 illustrates the effect of SF and stirrups on the confined SFRC stress-strain curve. As illustrated in this figure, increasing the steel fiber volume percentage enhances the initial stiffness, the peak confined concrete stress and the corresponding strain. Moreover, it was shown that for a higher SF volume percentage, the slope of the descending branch roughly approaches zero.



(a) Influence of steel fiber



(b) Influence of stirrups volume ratio

Fig. 1 Confined SFRC stress-strain curve

3.3 Behavior of SFRC in tension

To calculate the stress-strain relationship in tension for SFRC, in this study, the models previously developed by Campione and Mangiavillano (2008) and Lok and Xiao (1998) are used. The stress-strain relationship includes three linear branches. This curve was considered as an initial ascending branch up to the peak tension stress, which is proposed by Lok and Xiao (1998) f_{ctf} (the corresponding strain is ε_{ctf}), the second branch descends to the residual strength f_r and it is assumed to be constant from the point of the coordinate ε_{ctu} to the strain of 0.02 (Lok and Xiao 1998) in the third branch.

$$\sigma = \begin{cases} \varepsilon_t E_{ctf} & \text{for } \varepsilon_t < \varepsilon_{ctf} \\ (f_{ctf} - f_r) \left[\frac{\varepsilon_t - \varepsilon_{ctf}}{\varepsilon_{ctu} - \varepsilon_{ctf}} \right] + f_r & \text{for } \varepsilon_{ctf} < \varepsilon_t < \varepsilon_{ctu} \\ f_r & \text{for } \varepsilon_{ctu} < \varepsilon_t < 0.02 \end{cases} \quad (15)$$

in which

$$f_{ctf} = f_m (1 - v_f) + \frac{\eta \tau_d v_f L_f}{D_f} \quad (16)$$

$$f_m = 0.292 \sqrt{f_c'} \quad (17)$$

$$\varepsilon_{ctu} = 2 f_{yh} \left(\frac{1}{E_s} + \frac{\rho_t}{E_0} \right) \quad (18)$$

$$f_r = 0.2 \sqrt{f_c'} F \quad (19)$$

where E_s is the stirrups elasticity modulus, ρ_t is reinforcing steel ratio in the transverse direction, f_m is the concrete tension stress (MacGregor et al. 1960), η is the fiber orientation (which is taken as 0.5) and τ_d is the bond stress (=4.15 (choi et al. 2007)), respectively. E_{ctf} is the modulus of elasticity in tension.

As demonstrated in Fig. 2, an increase in the volume percentage of steel fiber improves SFRC characteristics in tension (note that the curve is plotted up to the strain of 0.002).

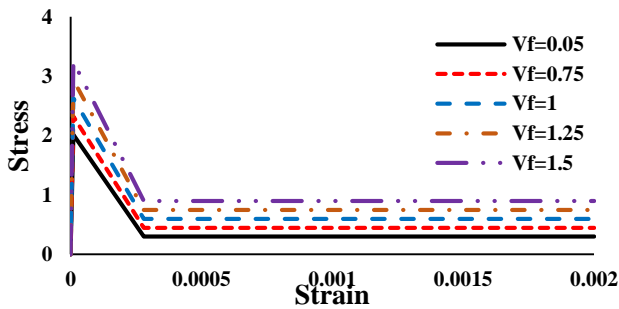


Fig. 2 Assumed stress-strain curve for SFRC in tension

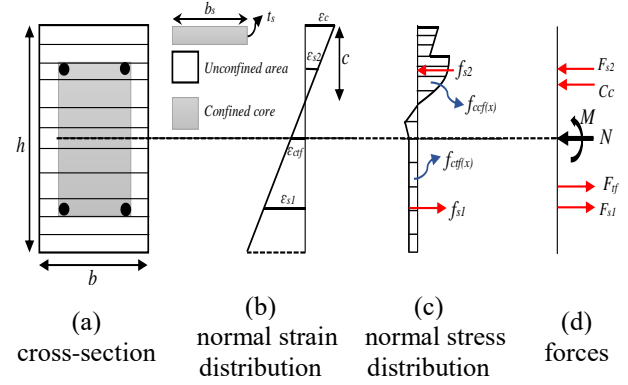


Fig. 3 Fiber analysis of a SFRC section

4. Nonlinear analysis of RC beams and columns with SF

4.1 Moment-curvature relationship for SFRC section

In this section, procedures for the calculation of moment-curvature relationship in RC beam/column sections with SF, following a fiber method, will be addressed. As shown in Fig. 3, for a given section, moment-curvature analysis is calculated based on the principles of strain compatibility and equilibrium and material constitutive relations for steel and concrete.

The required steps for the estimation of the moment-curvature relationship are briefly described below:

- 1- Assumption of a value for the strain at the top layer of the compression zone
- 2- Assumption of a value for the neutral axis
- 3- Calculate the compression and tension forces caused by the concrete and steel bars following the developed stress-strain models for SFRC and steel.
- 4- Control the force equilibrium in the section, following Eq. (20). If the value of $C_c + F_{si} + F_{tf}$ is close to the value of the axial load, the depth of the neutral axis is correctly assumed, otherwise the new value should be assumed for the neutral axis.

$$C_c + F_{si} + F_{tf} - N = 0 \quad (20)$$

- 5- Calculate the flexural moment, as presented in the following equation

$$M_f = \sum f'_c(x) b_s t_s x_i + \sum F_{si} d_i + \sum f_{tf}(x) b_s t_s x_i \quad (21)$$

where x_i and d_i are respectively the distances of the concrete strips and steel bars to the neutral axis.

- 6- Calculate the corresponding curvature, following Eq. (22)

$$C_c + F_{si} + F_{tf} - N = 0 \quad (22)$$

- 7- Assume a new strain at the peak of the compression zone. The analysis is stopped when any fracture occurs (e.g., fracture in compression zone, buckling of longitudinal bars (Berry and Eberhard 2005), etc.).
- 8- Calculate the effective flexural rigidity using Eq. (3)

when the tension bars yield.

Fig. 4 demonstrates that increasing in steel fiber volume percentage results in an increasing in the stiffness of the section.

In order to perform a nonlinear analysis, moment-rotation relationship would be required. Herein the curvature-rotation relationship is determined based on the plastic hinge formation (Bae and Bayrak 2008). To determine the rotational characteristics of a cantilever member corresponding to the generated shear force, V , according to the assumed curvature distribution as shown in Fig. 5, calculation of the rotation at the end of the member is given bellow

$$\theta_i = \frac{\varphi_i L_{eff}}{2} \quad \text{for } \varepsilon_s < \varepsilon_y \quad (23)$$

$$\theta_i = \theta_y + (\varphi_i - \varphi_y) L_p \quad \text{for } \varepsilon_s \geq \varepsilon_y \quad (24)$$

$$L_{eff} = L + 0.022 f_s d_b \quad f_s \leq f_y \quad (25)$$

where L_p is the plastic hinge length. Pauley and Priestley (1992) proposed Eq. (26) to calculate L_p for RC members. Because there is no conventional relationships to estimate the length of the plastic hinge for SFRC beams and columns, the length of the plastic hinge, L_p , recommended by Pauley and Priestly (1992) is used as follows

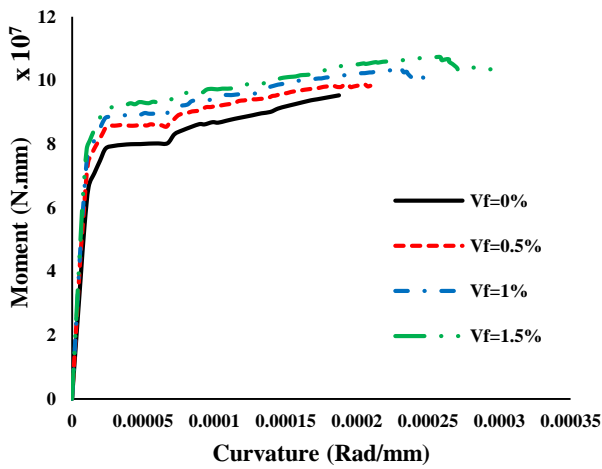


Fig. 4 Effect of SFRC on moment-curvature diagram

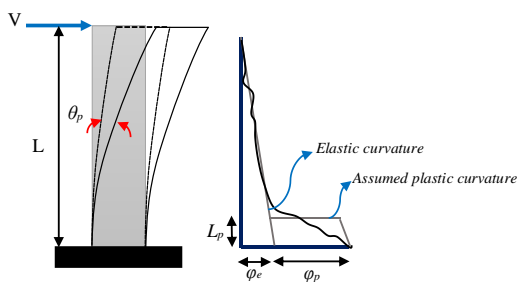


Fig. 5 Plastic hinge analysis

$$L_p = kL + 0.022 f_y d_b \leq 0.044 f_y d_b \quad (26)$$

$$k = 0.2 \left(\frac{f_{su}}{f_y} \right) - 1 \leq 0.08 \quad (27)$$

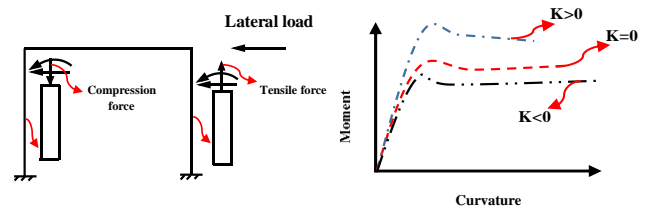
where f_{su} is the peak strength of the steel and d_b is the diameter of the longitudinal bar, respectively, and L is the length between maximum and the point of contra-flexure.

4.2 Varying axial load

Axial load is one of the most significant parameters that affect the nonlinear behavior of RC columns. Fig. 6 shows the exterior columns' axial load variation of a frame caused by the applied lateral load. It shows that by increasing the lateral load, the tensile and compression axial loads will be respectively subtracted from and added to the gravity load in two opposite sides of the frame. Accordingly, when the compression axial load decreases, the location of the neutral axis is transferred toward the top compressive layer of the section. Therefore, the reduction in the effective area of the cracked section is obtained, which will result in the reduction of the effective flexural rigidity. Furthermore, when the compression axial load increases, the location of the neutral axis is transferred toward the bottom tensile layer of the section and causes an increase in the RC columns' effective flexural rigidity (Fig. 6(b)). According to the above discussion, the total axial load in each step can be written as

$$N = N_g + KV_c = N_g + K \frac{M_f}{L} \quad (28)$$

where N_g is gravity load, V_c is shear force during each steps due to the lateral load, M_f is the flexural moment and K is the column's varying axial load coefficient, respectively. According to Eq. (28), the value of $K.M_f/L$ is added to the gravity load in which K is positive for the columns under compression load and negative for the columns under tensile load resulting from the lateral load.



(a) Effect of lateral load on the applied axial load on column

(b) Effect of varying axial load on the nonlinear behavior of RC/SFRC column

Fig. 6 Varying axial load effects

According to the above discussion, the positive varying axial load coefficient results in a higher effective flexural rigidity and the negative varying axial load coefficient results in a lower effective flexural rigidity than that of columns with constant axial loads. In this paper, the effect of varying axial loads is considered as per the analytical model presented by Shayanfar and Akbarzadeh (2016, 2017).

5. Verification of the proposed model with experimental results

As discussed above, the analytical model is proposed to investigate the nonlinear behavior of RC beams and columns with SF. Herein, the results of the proposed analytical model is compared to the results of the experimental tests conducted by previous researchers, as mentioned in the following section. In this paper, the frames are modelled in SAP 2000 (2008) program and the lumped plasticity model with plastic hinges at both ends of a member is used for the purpose of nonlinear analysis. Whereas shear deformation in these types of elements is negligible, therefore it's not considered but P_Delta effect is considered in the modelled frame.

5.1 The columns tested by Germano *et al.* (2013)

Germano *et al.* (2013), conducted experimental tests to investigate the behavior of RC and SFRC columns under constant axial load and cyclic lateral load. In this test, height of each column was 1800 mm and the height of lateral loading was 1565 mm. Dimension of the cross section was 300 × 300 mm. The concrete compression strength of RC and SFRC were 51.9 and 42.1 MPa, respectively. SFRC specimens contains 1 percent SF content. Specimen P07 contains plain concrete and P15 contains SFRC. Stirrups with 6 mm diameter were used for P07 and P15. Specimen P07 has 80 mm stirrups spacing and P15 has 100 mm stirrups spacing. Constant axial load of 190 KN was applied. Fig. 7 shows the geometry of the column and loading. The envelope curves of the specimens is given in Fig. 8. The results of the proposed analytical model and experimental tests are compared. The results indicate that the nonlinear behavior of RC and SFRC columns can be predicted by the proposed analytical model very well. Also they show that the members' initial stiffness, which depends on flexural rigidity of each member, can be accurately predicted with the proposed analytical procedure. Moreover, the strength and ultimate displacement predicted by the analytical model had good agreements with the results of the experimental tests.

5.2 The beams tested by Ashour *et al.* (2000)

Ashour *et al.* (2000), conducted experimental tests to investigate the effect SF on the RC beams capacity. The beams were constructed with the overall length of 3080 mm. All beams were nominally 200 mm wide and 250 mm deep. The concrete compression strength with normal,

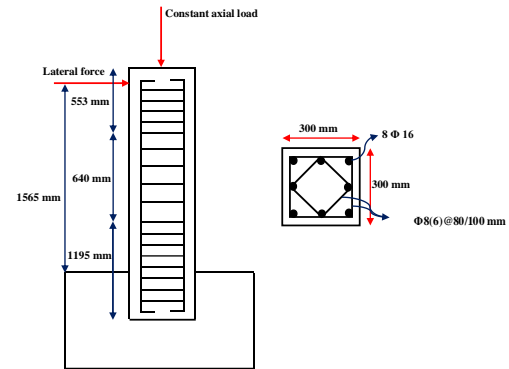


Fig. 7 Geometry and loading of the tested RC column of Germano *et al.* (2013)

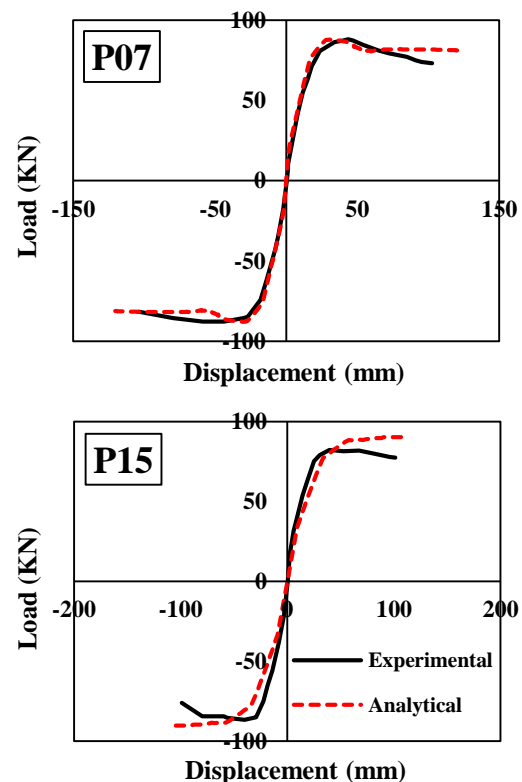
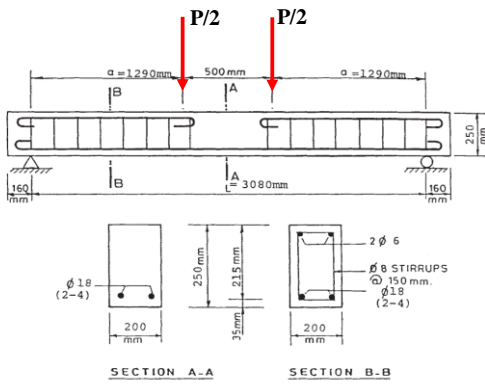
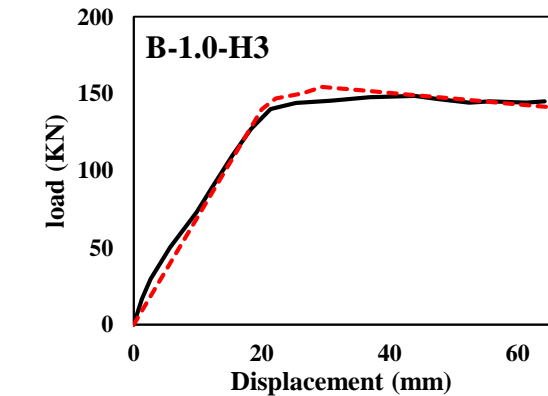
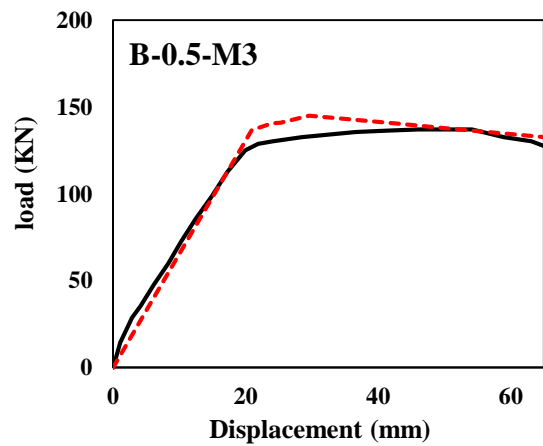
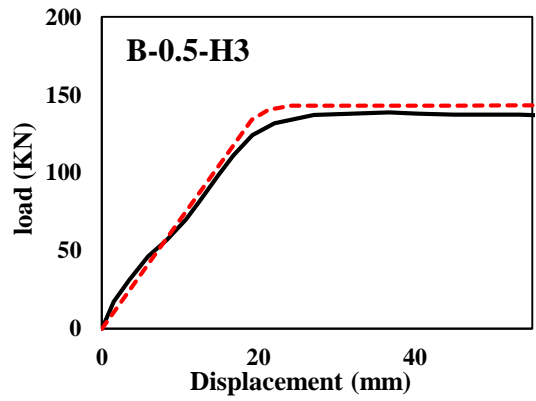
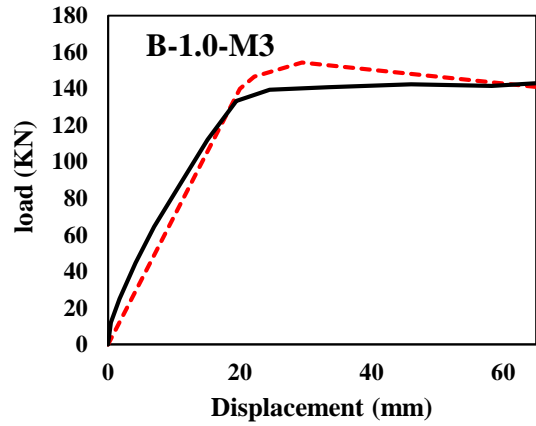
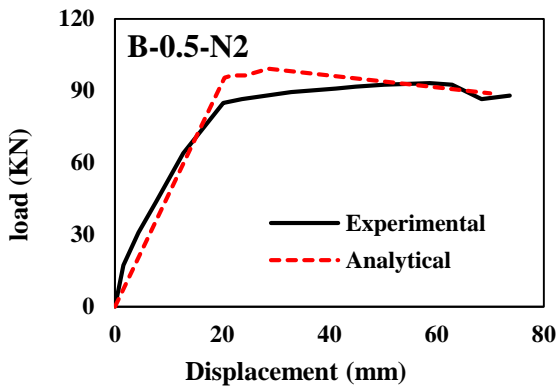


Fig. 8 Result of the analytical model and the experimental RC and SFRC columns of Germano *et al.* (2013)

medium and high strength of specimens were 49, 79 and 102 MPa, respectively. Also the fiber percentage of 0.5 and 1 is used. Fig. 9(a) shows the experimental beams and the applied load. The monotonic 4-point load is applied at the upper face of the beams. The load-displacement curves derived from the experimental tests and the analytical model are plotted in Fig. 9(b). For example, specimen B-0.5-N3 represents the characteristics of the beam with 0.5 percent SF content and normal concrete with three 18 mm longitudinal bars. According to this figure, the initial stiffness of the load-displacement curve for the beams can be accurately predicted using the proposed analytical model. Also, this model can precisely predict the strength and the ultimate displacement of the beams.



(a) Experimental beams detail



(b) Result of the analytical model and the experimental beams

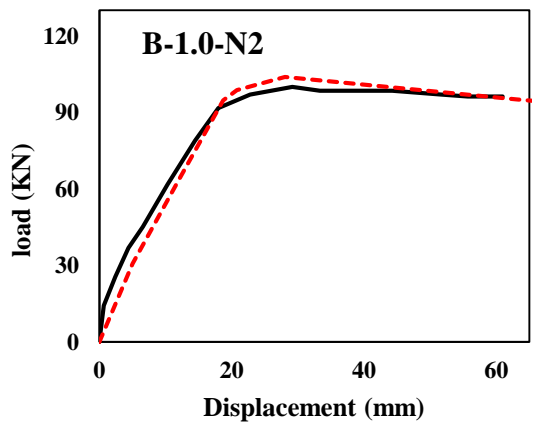
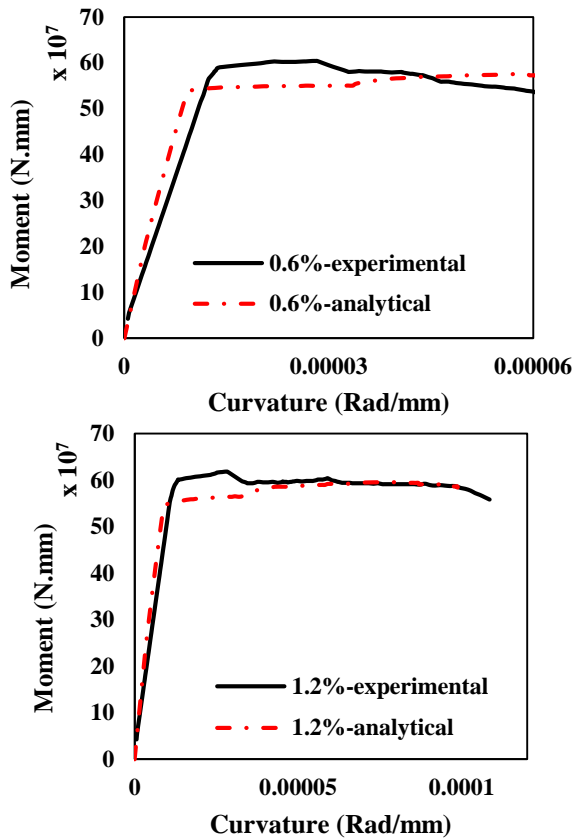
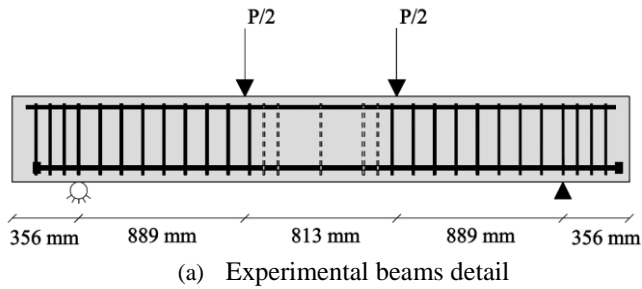


Fig. 9 Beams tested by Ashour et al. (2000)

5.3. The beams tested by Monfardini et al. (2015)

Monfardini *et al.* (2015), conducted experimental tests on SFRC beams to determine the SF effect on the plastic behavior of the beams at the onset of the compressed bars buckling. All beams were nominally 460 mm wide and 460 mm deep. The concrete compression strength was 36 MPa. Two beams with SF volume percentage of 0.6 and 1.2 were tested. The four point monotonic load was applied at the top of the beams. Fig. 10(a) shows the experimental beam and the applied load. The result of the experimental test and proposed analytical model is given in Fig. 10(b). Comparing the results of the proposed analytical model and experimental test shows that the initial stiffness, moment and ultimate curvature of the moment-curvature curve of



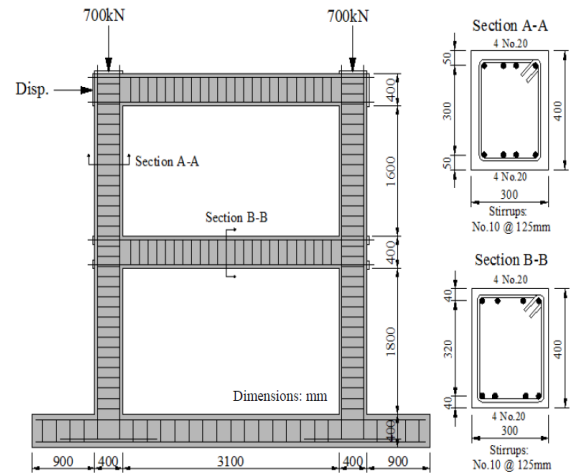
(b) Result of the analytical model and the tested beams

Fig. 10 Beams tested by Monfardini *et al.* (2015)

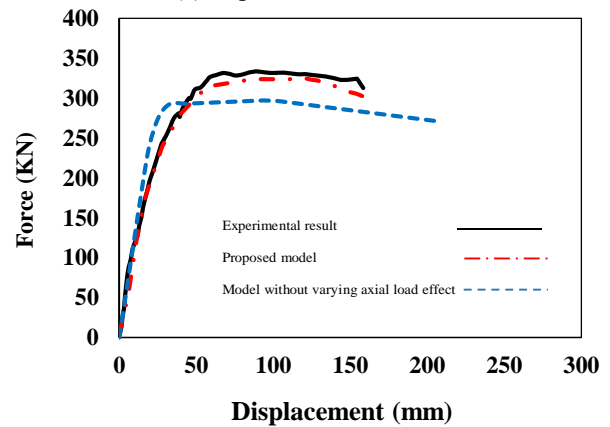
the beams can be predicted with proposed analytical accurately.

5.4 The frame tested by Vacchio and Emara (1992)

Vacchio and Emara (1992), investigated the flexural capacity of RC frame. The 2-story frame was built with a center-to-center span of 3500 mm, height of story was 2000 mm and an overall height of 4600 mm. Dimensions of the beams and columns were 300 mm wide and 400 mm deep. The concrete compression strength of RC was 30 MPa. Also, the constant axial load of 700 KN was applied at the top of each column of the second story. The monotonic lateral load was applied at the top of the second story. Fig. 11(a) shows the experimental frame setup and the applied load. The load-displacement curves derived from the experimental tests and the analytical model are plotted in Fig. 11(b). According to this figure, the initial stiffness of



(a) Experimental frame details



(b) Result of the analytical model and the experimental frame

Fig. 11 Tested frame of Vecchio and Emara (1992)

the load-displacement curve of the frame can be accurately predicted with the analytical model. In this frame, the effect of the varying axial load is also considered, which again confirms the accuracy of the proposed model.

Figs. 8-11 show approximately accurate prediction of the behavior of the RC and SFRC members and frames using the analytical procedure in terms of stiffness, strength (or moment) and the ultimate displacement (or curvature).

Using the proposed analytical model, the flexural rigidity reduction factor, α_{eff} , of various SFRC sections with different variables is also investigated and presented in the following section.

6. Parametric study and proposed equation for α_{eff}

To investigate the SF effects on the effective flexural rigidity of reinforced normal-strength concrete (which are the structural concrete and the strain corresponds to the peak stress is about 0.002 and the post peak of stress-strain curve shows ductile behavior) beams and columns, a parametric study is conducted with different variables such as concrete compressive strength, constant axial load ratio, varying axial load coefficient, longitudinal bars percentage,

Table 2 Parameter range for various SFRC column section

Parameters	Range	
	Min	Max
$v=N/A_g f_c$	0	0.5
f_c (MPa)	20	50
ρ_t	0.01	0.04
K	-4	4
v_f (%)	0	1.5

ρ_t is longitudinal bars percentage

Table 3 Parameter range for various SFRC beams section

Parameters	Range	
	Min	Max
ρ_{st}	0.005	0.02
f_c (MPa)	20	50
ρ' / ρ_{st}	0	1
v_f (%)	0	1.5

ρ_{st} is tension bars percentage; ρ' is compression bars percentage

etc., as listed in Tables 2 and 3. A total of 3398 rectangular RC/SFRC columns and 1155 rectangular RC/SFRC beam sections are analyzed and the effective flexural rigidity is calculated according to Eq. (3). The effects of these variables on the effective flexural rigidity are evaluated by calculating the dimensionless reduction factor α_{eff} . In the following section, the effects of each parameter is discussed.

6.1 Effect of longitudinal bars percentage

Fig. 12(a) shows the effect of longitudinal bars percentage (ρ_t) on the effective flexural rigidity of columns. Concrete compressive strength of 20 MPa, section dimensions of 450×450 mm and the axial load ratio of 0.123 assumed to be constant. The results indicate that by increasing in ρ_t , α_{eff} increased and vice versa. According to the obtained results, α_{eff} increased 6.5, 11.2, 20.2 and 24.2 percent with steel fiber volume percentage of 0.5, 0.75, 1.25 and 1.5 percent in comparison with RC columns without SF. Comparing the α_{eff} proposed by ACI318 and CSA A23.3 with the obtained results show that the α_{eff} of the RC column with 3% longitudinal bars and the column with 1.5% SF volume percentage and 2.2% longitudinal bars had good agreement with the value which is proposed by ACI318 and CSA A23.3.

As shown in Figs. 13(a) and 13(c), increasing both tension and compression bars percentage in RC/SFRS beams results in an increase in α_{eff} . Accordingly, concrete compressive strength of 30 MPa, section dimensions of 300×300 mm assumed to be constant. Comparing α_{eff} proposed by ACI318 and CSA A23.3 with the results obtained from the proposed model indicates that this factor for the RC beam with 0.85% tension bars and the beam with 1.5% SF volume percentage and 0.6% tension bars is close to the estimated values by ACI318 and CSA A23.3.

6.2 Effect of varying axial load coefficient

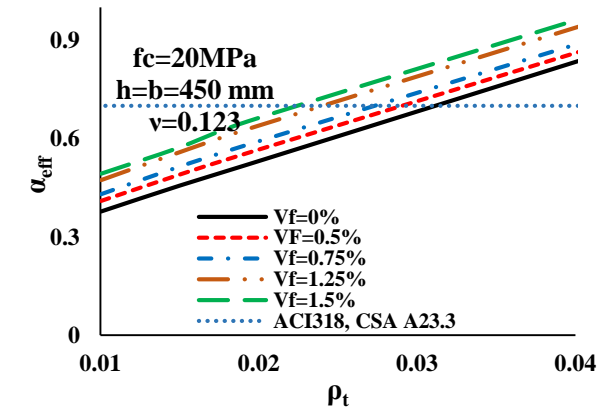
Fig. 12(b) shows the effect of varying axial load coefficient (K) on α_{eff} . The calculated results show that by increasing the K , α_{eff} increased and vice versa. According to the calculated results, α_{eff} increased by 4.7, 10.4 and 16.4 percent with steel fiber volume percentage of 0.5, 1 and 1.5 percent in comparison with the RC columns without SF. Concrete compressive strength of 25 MPa, section dimensions of 450×450 mm, axial load ratio of 0.098, and longitudinal bars percentage of 3.18% are assumed to be constant. It can be seen that in the given section, α_{eff} of the RC column with the varying axial load coefficient of 4 and the RC column with 1.5% SF volume percentage and the varying axial load coefficient of -2.5 is nearly similar to the values recommended by ACI318 and CSA A23.3.

6.3 Effect of the axial load ratio

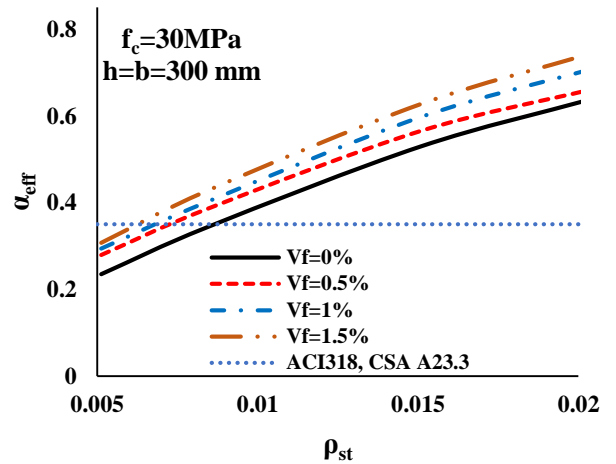
Fig. 12(c) shows the effect of axial load ratio (v) on α_{eff} . The results show that by increasing the v , α_{eff} increased. According to the obtained results, α_{eff} increased by 4.4, 8.8 and 13.3 percent with steel fiber volume percentage of 0.5, 1, and 1.5 percent in comparison with the RC columns without SF. According to the obtained results of the parametric study, in higher axial load level M_y depended on the nonlinearity of the concrete (concrete strain reaches 0.002). As it is shown in Fig. 12(c), concrete compressive strength of 25 MPa, section dimensions of 450×450 mm, and longitudinal bars percentage of 3.18% are assumed to be constant. According to the given section, α_{eff} of the RC column with the axial load ratio of 0.3 and the RC column with 1.5% SF volume percentage and the axial load ratio of 0.1 is approximately similar to the values recommended by ACI318 and CSA A23.3.

6.4 Effect of concrete compressive strength

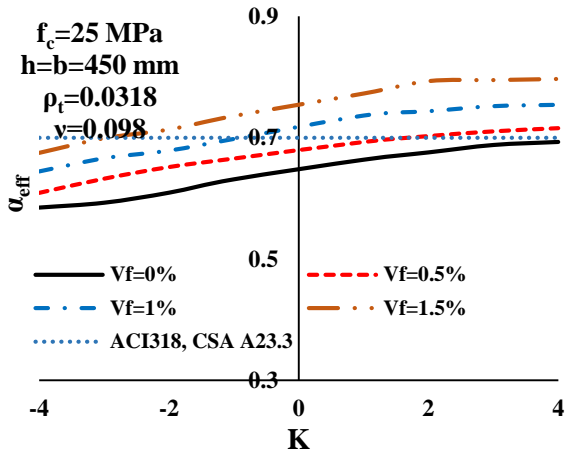
Increasing the concrete compressive strength results in a reduction in α_{eff} for RC/SFRC columns and beams (Figs. 12(d) and 13(b)). The calculated results show that by increasing the concrete compressive strength, the ratio of yield moment to the yield curvature increased, on the other hand, by taking into account the relationship among concrete compressive strength and its modulus of elasticity ($E_c = wc1.50.043\sqrt{f_c}$, wc is the concrete weight), according to Eq. (1), a reduction in α_{eff} is obtained. As it is shown in Figs. 12(d) and 13(b), higher concrete compressive strength the effect of the steel fiber decreased. According to the calculated results, α_{eff} increased by 2.1, 6.8 and 12 percent with the steel fiber volume percentage of 0.5, 1, and 1.5 in comparison with the RC columns without SF (according to Fig. 12(d)). According to Figure 12d, section dimensions of 450×450 mm, longitudinal bars percentage of 3.18%, and axial load of 1500 KN are assumed to be constant. According to the given section, α_{eff} of the RC column with the concrete compressive strength of 25 MPa and the RC column with 1.5% SF volume percentage and concrete compressive strength of 43 Mpa have good agreement with such values recommended by ACI318 and CSA A23.3.



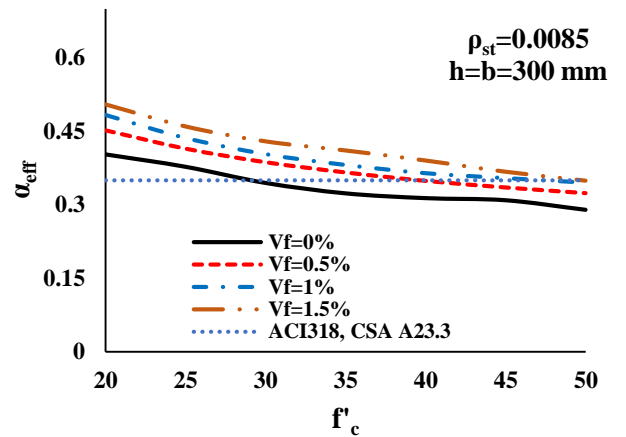
(a) effect of longitudinal bars percentage



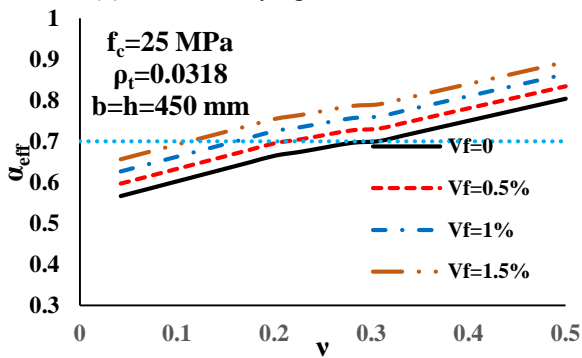
(a) effect of tension bars percentage



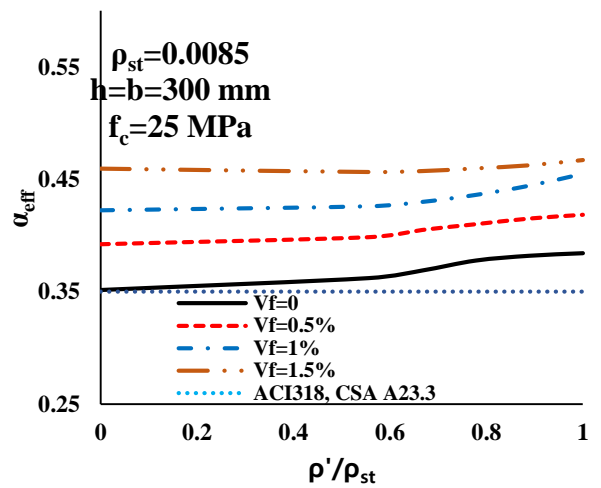
(b) effect of varying axial load coefficient



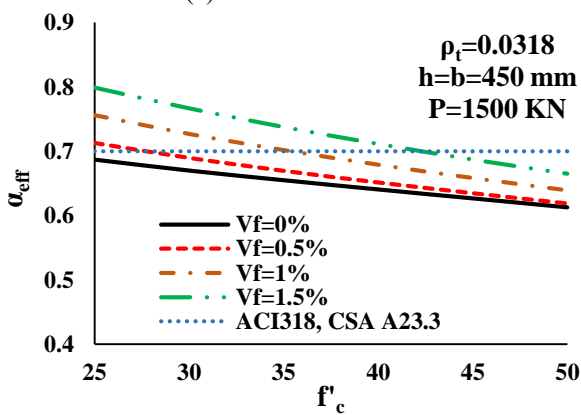
(b) effect of concrete compressive strength



(c) effect of axial load ratio



(c) effect of compression to tension bars ratio



(d) effect of concrete compression strength

Fig. 12 Effective of various factor on α_{eff} of column sections with different steel fiber volume percentage

Fig. 13 Effective of various factor on α_{eff} of beams sections with different steel fiber volume percentage

This conclusion can be obtained from Fig. 13(b) for RC beams with SF. Moreover, it can be seen that in higher concrete compressive strength, the effect of SF decreased.

6.5 Effect of steel fiber percentage

According to the results shown in Figs. 12 and 13, increasing the fiber percentage increase the α_{eff} . According to Fig. 12© in higher axial load ratio, the effect of steel fiber on α_{eff} increased. Moreover, it is noted that by increasing the concrete compressive strength, the effect of steel fibers decreased and in lower concrete compressive strength had more effect on α_{eff} (Figs. 12(d) and 13(b)).

According to the above results, increasing in axial load ratio, ν , longitudinal bars percentage, ρ_l , varying axial load coefficient, K and SF volume percentage increased α_{eff} . Moreover, increasing the concrete compression strength f'_c , decreased α_{eff} . To identify the RC columns section with steel fiber, a limiting ν based on ρ_l is defined (Avşar *et al.* 2014). Accordingly, Eqs. (29) and (30) are proposed to calculate α_{eff} for RC columns with SF through a linear regression analysis.

$$\alpha_{eff} = C_1 + C_2 f'_c + C_3 K + C_4 \rho_l + C_5 \nu + C_6 F, \nu = \frac{N}{A_g f'_c} > 0.3 - 1.91 \rho_l \quad (29)$$

$$\alpha_{eff} = C'_1 + C'_2 f'_c + C'_3 K + C'_4 \rho_l + C'_5 \nu + C'_6 F, \nu \leq 0.3 - 1.91 \rho_l \quad (30)$$

where C_1 to C_6 are 0.105, 0.001, 0.017, 12.753, 0.537 and 0.116, and C'_1 to C'_6 are 0.196, -0.002, 0.015, 12.412, 0.62 and 0.068, respectively. The correlation coefficient is calculated as 0.961 which shows high accuracy.

As discussed previously, increasing the tension bars percentage, ρ_{st} , compression to tension bars ratio, ρ' / ρ_{st} , and SF volume percentage have an increasing effect and the concrete compressive strength, f'_c has a decreasing effect on α_{eff} . Therefore, Eq. (31) is proposed to calculate α_{eff} for RC beams with SF.

$$\alpha_{eff} = D_1 + D_2 f'_c + D_3 \rho_{st} + D_4 \frac{\rho'}{\rho_{st}} + D_5 F \quad (31)$$

where D_1 to D_5 are 0.268, -0.004, 25.65, 0.008 and 0.107, respectively. These coefficients are achieved through a linear regression. The correlation coefficient is calculated as 0.979 which shows high accuracy.

As an example a typical four story RC/SFRC moment resisting frame (containing 1% steel fiber) with three bays of 5 m and the height of 3 m is analyzed using nonlinear behavior of the sections through the proposed analytical model. To verify the proposed equations, this frame were analyzed using linear behavior of the sections considering the effective flexural rigidity based on Eqs. (29)-(31).

Table 4 Section details of the four story SFRC frame

frame	members	Floors	width	depth	reinforcement
4- story	Beams	1-2	450	450	6φ18top+4φ16bot
	Beams	3-4	400	400	5φ18top+3φ16bot
	Columns	1-2	450	450	16φ18
	columns	3-4	400	400	12φ16

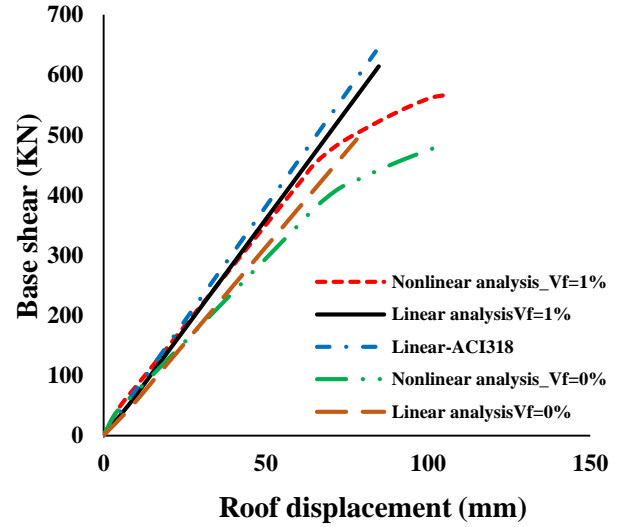


Fig. 14 Base shear- roof displacement curve of the four story frame

Moreover, a linear analysis was performed using effective flexural rigidity recommended by ACI318. Table 4 illustrates the cross-section details of this frame. Concrete compressive strength is assumed to be 20 MPa and the bars yield and ultimate strength are equal to 400 and 600 MPa, respectively. Fig. 14 shows the base shear-roof displacement curve of the study frame.

As it is shown in this figure, the frame containing steel fibers behaved stiffer than the frame without steel fibers which are analyzed through the proposed analytical model. It can be seen that stiffness of the RC/SFRC frames which are analyzed linearly using the effective flexural rigidity (based on the proposed equations) have good agreements with the stiffness of the frames analyzed through the proposed analytical model. Comparing the results of RC frame and the frame using ACI318 recommendations, indicated that the calculated stiffness of the RC frame using nonlinear analysis and the RC frame using code recommendations in linear analysis are not in good agreement. Therefore, this curve shows that the analyzed frame using ACI318 recommendations is not in the safety margin.

7. Conclusions

This paper presents an analytical nonlinear analysis to predict the nonlinear behavior of RC columns and beams with SF. Moreover, an analytical procedure is proposed to predict the nonlinear behavior of RC frames with SF. This paper also presents the equations to calculate the effective flexural rigidity of RC beams and columns with steel fibers. The proposed equations have been developed on the basis of the parametric analysis of a comprehensive set of RC beams and columns with SF. Variables such as steel fiber volume percentage, axial load ratio, varying axial load coefficient, concrete compressive strength, and longitudinal bars percentage are considered. The conclusions from this study are summarized below.

The proposed analytical model can predict the nonlinear behavior of RC and SFRC members very well. Accordingly, in addition to the axial load ratio, the amount of longitudinal bars and concrete compressive strength, varying axial load and steel fiber volume percentage have been identified as the most important variables affecting the section yield point as well as the effective flexural rigidity of the section. High varying axial load coefficient increases the effective flexural rigidity. Moreover, increasing in steel fiber volume percentage increases the effective flexural rigidity. It is obtained that the current codes such as ACI318 and CSA A23.3 in some cases overestimate the α_{eff} values for low longitudinal bars and axial load. The verification of the proposed equations indicates that the stiffness of the RC/SFRC frames predicted by the proposed analytical model were in good agreement with the stiffness of the RC/SFRC frames predicted with the linear analysis based on the proposed equations for α_{eff} . Also, comparing the results of RC frame and the frame using ACI318 recommendations, indicated that the calculated stiffness of the RC frame using nonlinear analysis and the RC frame using code recommendations in linear analysis are not in good agreement.

References

- Abbass, W., Khan, M.I. and Mourad, S. (2018), "Evaluation of mechanical properties of steel fiber reinforced concrete with different strengths of concrete", *Constr. Build. Mater.*, **168**, 556-569.
- Abrams, D.P. (1987), "Influence of axial force variations on flexural behavior of reinforced concrete columns", *Struct. J.*, **84**(3), 246-254.
- ACI (American Concrete Institute). (2014). Building Code Requirements for Structural Concrete and Commentary, Standards ACI 318-14 and ACI 318R-14. Farmington Hills: Michigan.
- Ashour, S.A., Wafa, F.F. and Kamal, M.I. (2000), "Effect of the concrete compressive strength and tensile reinforcement ratio on the flexural behavior of fibrous concrete beams", *Eng. Struct.*, **22**(9), 1145-1158. [https://doi.org/10.1016/S0141-0296\(99\)00052-8](https://doi.org/10.1016/S0141-0296(99)00052-8).
- Avsar, Ö., Bayhan, B. and Yakut, A. (2014), "Effective flexural rigidities for ordinary reinforced concrete columns and beams", *Struct. Des. Tall Spec. Build.*, **23**(6), 463-482. <https://doi.org/10.1002/tal.1056>.
- Bae, S. and Bayrak, O. (2008), "Plastic hinge length of reinforced concrete columns", *ACI Struct. J.*, **105**(3), 290.
- Bae, B.I., Choi, H.K., Lee, M.S. and Choi, C.S. (2017), "Indirect tensile strength of UHSC reinforced with steel fibres and its correlation with compressive strength", *Mag. Concrete Res.*, **69**(15), 772-786. <https://doi.org/10.1680/jmacr.15.00545>.
- Berry, M.P. and Eberhard, M.O. (2005), "Practical performance model for bar buckling", *J Struct Eng.*, **131**(7), 1060-1070. [https://doi.org/10.1061/\(ASCE\)0733-9445\(2005\)131:7\(1060\)](https://doi.org/10.1061/(ASCE)0733-9445(2005)131:7(1060)).
- Campione, G. and Mangiavillano, M.L. (2008), "Fibrous reinforced concrete beams in flexure: experimental investigation, analytical modelling and design considerations", *Eng. Struct.*, **30**(11), 2970-2980. <https://doi.org/10.1016/j.engstruct.2008.04.019>.
- Chalioris, C.E. and Panagiotopoulos, T.A. (2018), "Flexural analysis of steel fibre-reinforced concrete members", *Comput. Concrete*, **22**(1), 11-25. <https://doi.org/10.12989/cac.2018.22.1.011>.
- Chen, L., Liu, S.W. and Chan, S.L. (2017), "Divergence-free algorithms for moment-thrust-curvature analysis of arbitrary sections", *Steel Compos. Struct.*, **25**(5), 557-569. <https://doi.org/10.12989/scs.2017.25.5.557>.
- Choi, K.K., Hong-Gun, P. and Wight, J.K. (2007), "Shear strength of steel fiber-reinforced concrete beams without web reinforcement", *ACI Struct. J.*, **104**(1), 12.
- Computer and Structures Inc (2008), SAP2000 analysis references, Berkeley, California
- CSA. (2014), Design of Concrete Structures, CSA Standard A23.3-14. Canadian Standards Association: Mississauga, Ontario
- Gao, D.Y., You, P.B., Zhang L.J. and Yan, H.H. (2018), "Seismic behavior of SFRC shear wall with CFST columns", *Steel Compos. Struct.*, **28**(5), 527-539. <https://doi.org/10.12989/scs.2018.28.5.527>.
- Germano, F., Plizzari, G.A. and Tiberti, G. (2013), "Experimental study on the behavior of SFRC columns under seismic loads", *Proceedings of the 8th international conference on fracture mechanics of concrete and concrete structures*.
- Gribniak, V., Kaklauskas, G., Kwan, A.K.H., Bacinskas, D. and Ulbinas, D. (2012), "Deriving stress-strain relationships for steel fibre concrete in tension from tests of beams with ordinary reinforcement", *Eng. Struct.*, **42**, 387-395. <https://doi.org/10.1016/j.engstruct.2012.04.032>.
- Jang, S.J. and Yun, H.D. (2018), "Combined effects of steel fiber and coarse aggregate size on the compressive and flexural toughness of high-strength concrete", *Compos. Struct.*, **185**, 203-211. <https://doi.org/10.1016/j.compstruct.2017.11.009>.
- Kumar, R. and Singh, Y. (2010), "Stiffness of Reinforced Concrete Frame Members for Seismic Analysis.", *ACI Struct. J.*, **107**(5), 607-615.
- Lee J.H., Cho B. and Choi, E. (2017), "Flexural capacity of fiber reinforced concrete with a consideration of concrete strength and fiber content", *Constr. Build. Mater.*, **138**, 222-231. <https://doi.org/10.1016/j.conbuildmat.2017.01.096>.
- Lok, T.S. and Xiao, J.R. (1998), "Tensile behaviour and moment-curvature relationship of steel fibre reinforced concrete", *Mag. Concrete Res.*, **50**(4), 359-368. <https://doi.org/10.1680/mac.1998.50.4.359>.
- MacGregor, J.G., Sozen, M.A. and Siess, C.P. (1960), Strength and behavior of prestressed concrete beams with web reinforcement. University of Illinois Civil Engineering Studies, Structural Research Series 210, Urbana
- Mander, J.B., Priestley, M.J.N. and Park, R. (1988), "Observed stress-strain behavior of confined concrete", *J. Struct. Eng.*, **114**(8), 1827-1849. [https://doi.org/10.1061/\(ASCE\)0733-9445\(1988\)114:8\(1827\)](https://doi.org/10.1061/(ASCE)0733-9445(1988)114:8(1827)).
- Mirza, S.A. and Tikka, T.K. (1999), "Flexural stiffness of composite columns subjected to major axis bending", *Struct. J.*, **96**(1), 19-28.
- Monfardini, L., Lequesne, F., Minelli, G.J., Montesinos, P. and Pincheira, J.A. (2015), "Stability of reinforcing bars in steel fiber reinforced concrete flexural members", *Proceedings of the 7th International RILEM Conference on High Performance Fiber Reinforced Cement Composites (HPFRCC7)*. Stuttgart, Germany.
- Moradi, M., Bagherieh, A. and Esfahani, M.R. (2016), "Relationship of tensile strength of steel fiber reinforced concrete based on genetic programming", *Int. J. Optim. Civil Eng.*, **6**(3), 349-363.
- Ousalem, H., Kabeyasawa, T., Tasai, A. and Ohsugi, Y. (2002), "Experimental study on seismic behavior of reinforced concrete columns under constant and variable axial loadings", *Proceedings of the annual conference of Japan concrete institute*, Tsukuba, Japan.

- Paulay, T. and Priestley, M.N. (1992), Seismic design of reinforced concrete and masonry buildings.
- Priestley, M.N., Seible, F. and Calvi, G.M. (1996), Seismic design and retrofit of bridges. New York: John Wiley & Sons.
- Qissab, M.A. and Salman, M.M. (2018), "Shear strength of non-prismatic steel fiber reinforced concrete beams without stirrups", *Struct. Eng. Mech.*, **67**(4), 347-358. <https://doi.org/10.12989/sem.2018.67.4.347>.
- Sezen, H. (2002), Seismic behavior and modeling of reinforced concrete building columns, Ph.D., dissertation, University of California at Berkeley, Berkeley, CA.
- Shayanfar, J. and Bengar, H.A. (2016), "Numerical model to simulate shear behaviour of RC joints and columns", *Comput. Concrete*, **18**(4), 877-901.
- Shayanfar, J. and Bengar, H.A. (2017), "Nonlinear analysis of RC frames considering shear behaviour of members under varying axial load", *Bull. Earthq. Eng.*, **15**(5), 2055-2078. <https://doi.org/10.1007/s10518-016-0060-z>.
- Vecchio, F.J. and Emara, M.B. (1992), "Shear deformations in reinforced concrete frames", *ACI Struct. J.*, **89**(1), 46-56.
- Wang, Y.C. and Restrepo, J.I. (2001), "Investigation of concentrically loaded reinforced concrete columns confined with glass fiber-reinforced polymer jackets", *Struct. J.*, **98**(3), 377-385.
- Xu, C., Su, Q. and Masuya, H. (2017), "Static and fatigue performance of stud shear connector in steel fiber reinforced concrete", *Steel Compos. Struct.*, **24**(4), 467-479. <https://doi.org/10.12989/scs.2017.24.4.467>.
- Zarrin, O. and Khoshnoud, H.R. (2016), "Experimental investigation on self-compacting concrete reinforced with steel fibers", *Struct. Eng. Mech.*, **59**(1), 133-151. <https://doi.org/10.12989/sem.2016.59.1.133>.